Karlsruher Institut für Technologie

Finite Element study on semi-elliptical surface cracks in a cylinder

Open Access am KIT

by Gabriele Rizzi, Theo Fett

KIT SCIENTIFIC WORKING PAPERS 41

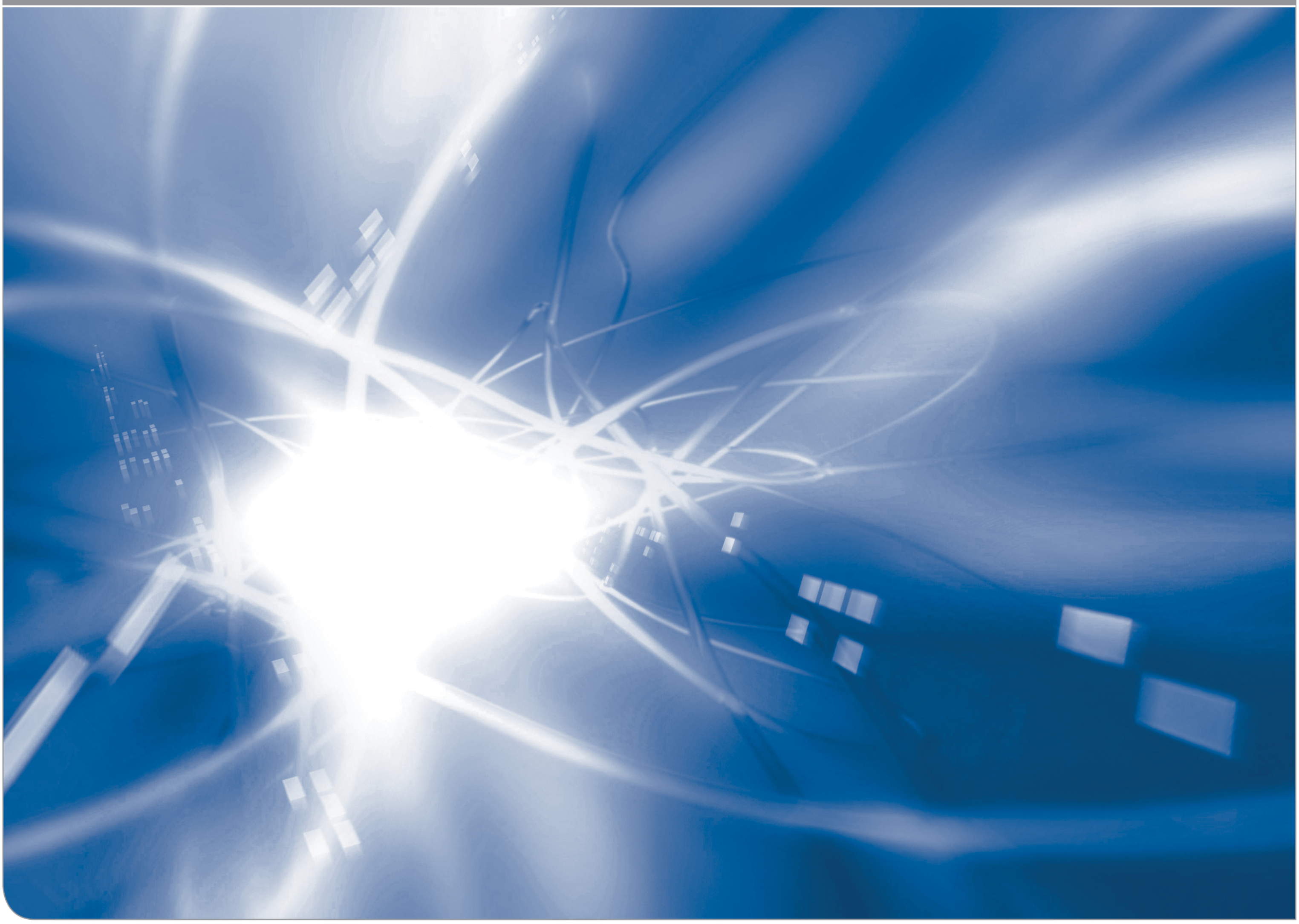

Institut für Angewandte Materialien, Karlsruher Institut für Technologie (KIT)

Impressum

Karlsruher Institut für Technologie (KIT)
www.kit.edu

2016

ISSN: 2194-1629

Abstract

Different types of test specimens were applied in the past for the measurement of subcritical crack growth in silica. The rather large scatter of crack-growth curves calls for re-analysis of stress intensity factors. In the present note semi-elliptical surface cracks in long cylinders are addressed. In addition the first regular stress term (T-stress) is considered.

Contents

1. Introduction

Different types of test specimens were applied in the past for the measurement of subcritical crack growth in silica. Figure 1 shows some crack growth results in water at room temperature obtained from literature. The crack-growth data by Wiederhorn and Bolz [1] were measured with the Double-Cantilever Beam (DCB) method. Michalske *et al.* [2] used the Double cleavage drilled compression (DCDC) specimen and Muraoka and Abe [3] carried out static tensile tests on silica fibres with small semi-elliptical surface cracks.

The data scatter is at a crack-growth rate of 10^{-7} m/s about 13% as indicated by the arrows in Fig. 1. In order to assess the results from [3] we performed Finite Element computations on semi-elliptical surface cracks in infinitely long cylinders. The results are given in this note.

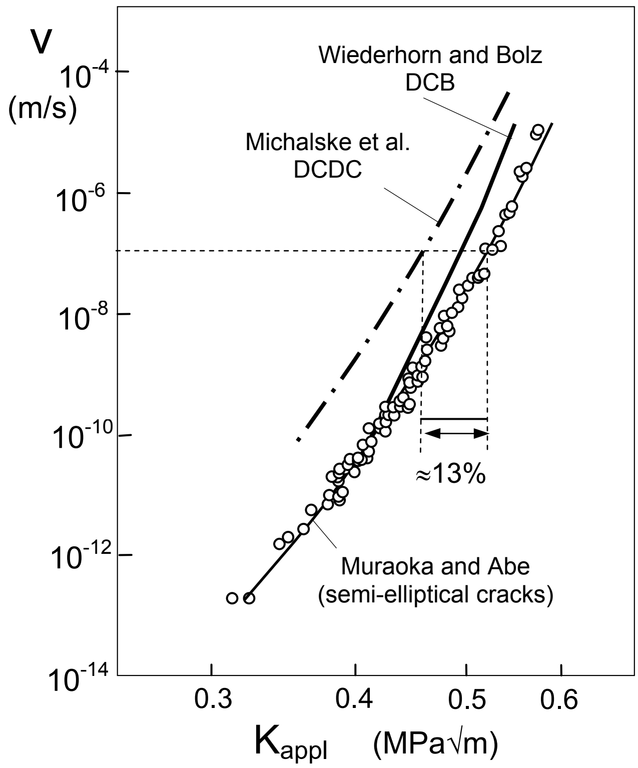

Fig. 1 Subcritical crack growth measurements on silica by Wiederhorn and Bolz [1] (DCB), Michalske et al. [2] (DCDC), , and Muraoka and Abe [3] (semi-elliptical surface cracks).

2. Stress intensity factors from literature

Literature results on the semi-elliptical crack in an infinitely long cylinder (see Fig. 2a) are available from Nisitani and Chen [4] and Shiratori et al. [5]. First, we compared the polynomial fit by Muraoka and Abe [3] with the literature data by Nisitani/Chen since both are using the Body-force method. The results are given in Fig. 2b in terms of the geometric function *F*, defined by

$$F = \frac{K}{\sqrt{\pi a}} \tag{1}$$

The polynomial approximation (curves) fits excellently to the open circles for ν=0.3 at a/c=0.5 and 1. Use of the value ν=0.3 (mostly used for handbook solutions of cracks in metals) was confirmed by Muraoka [6].
On the other hand, the Nisitani-data clearly show a considerable influence of the Poisson's ratio. This has to be considered for the computation of stress intensity factors for cracks in silica, showing a Poisson's ratio of ν=0.17.

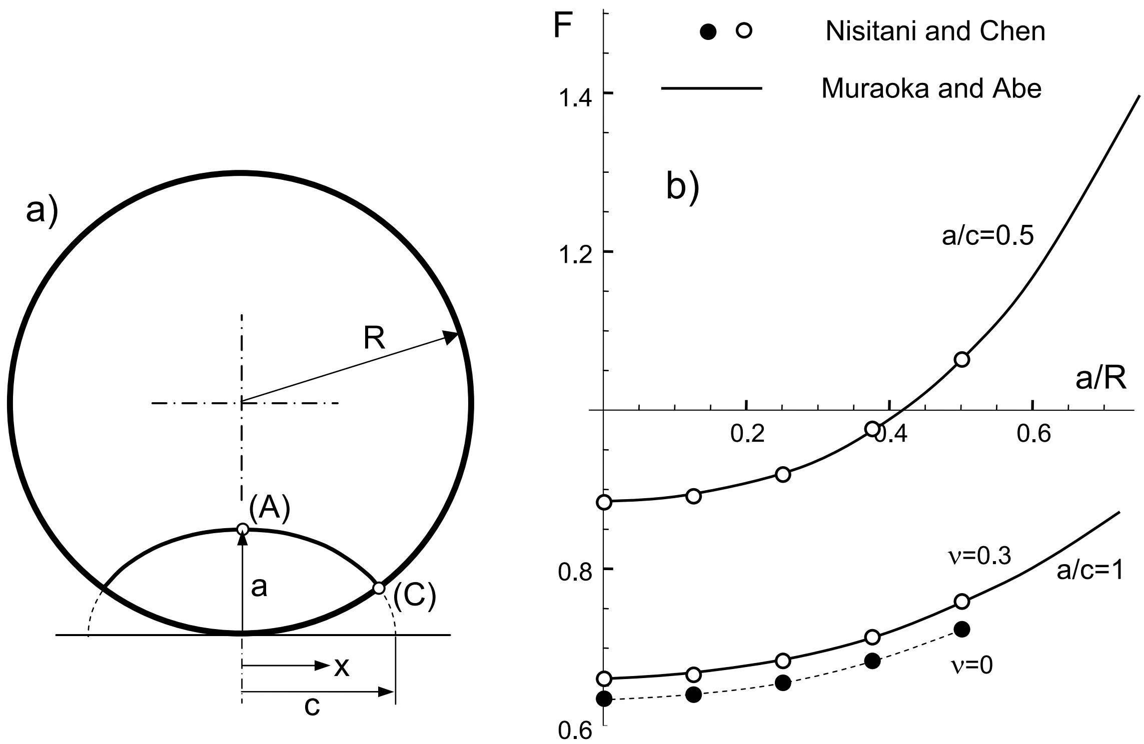

Fig. 2 a) Semi-elliptical surface crack in a cylinder, b) Geometric function F, symbols: results by Nisitani and Chen [4] for ν=0.3, solid lines: Fitting equation to results by Muraoka and Abe [3]. Maximum deviations between Nisitani and Chen and Muraoka and Abe for ν=0.3 are less than 0.5%.

In Fig. 3a the ratio of the Nisitani-data for ν=0 and 0.3 at a/c=1 is plotted against a/R. From this plot we see that the solution is about 4-5% smaller for ν=0. The values for the Poisson number of silica, ν=0.17, must be between ν=0 and 0.3. For our purpose the ratio of the stress intensity factors $K_{\nu=0.17}/K_{\nu=0.3}$ was of special interest because it allows a transformation of the crack-growth data by Muraoka et al. [3] using the correct stress intensity factors $K_{\nu=0.17}$.
Figure 3b shows the deviations between the Nisitani-solution and the equation from [3]. Best agreement is visible. The small deviations of less than 0.5% do nor show a trend with respect to a/R.

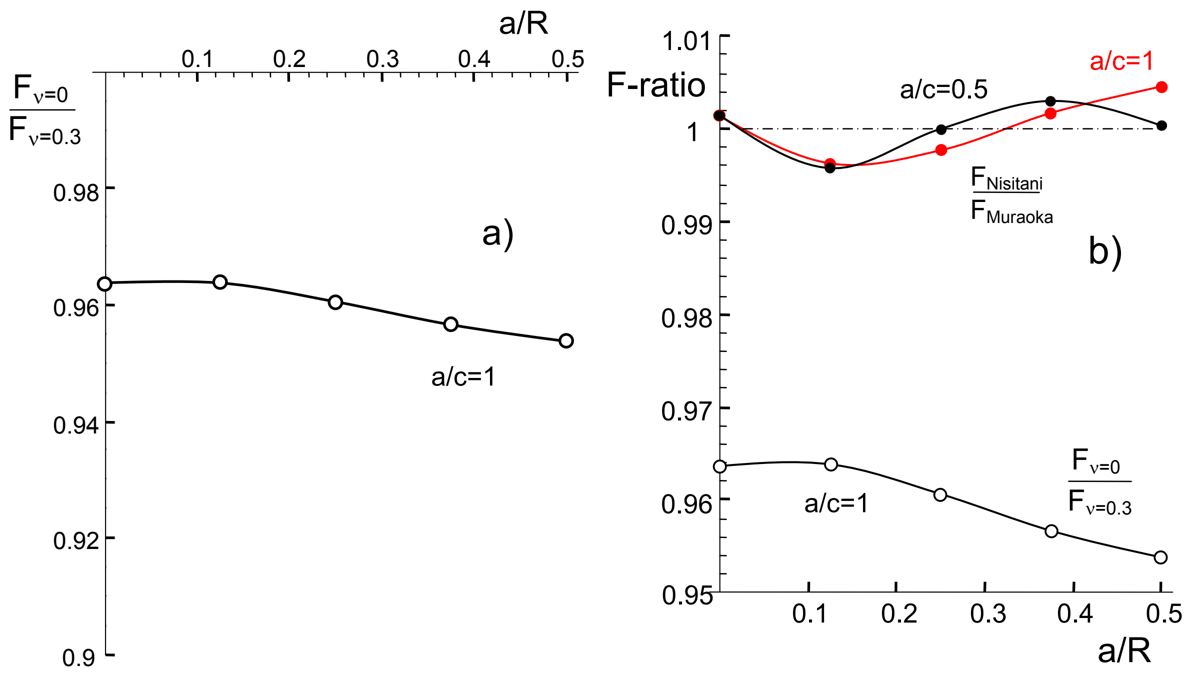

Fig. 3 a) Effect of Poisson's ratio on the geometric function for a/c=1, deviations up to 5%, b) deviations between Nisitani and Chen [4] for ν=0.3 and the fitting curve by Muraoka and Abe [3] for a/c=0.5 and a/c=1. Maximum deviations are less than 0.5%.

3. FE results

We computed stress intensity factors and T-stresses for semi-elliptical cracks by using Finite Elements. Since the cracks in [3] were within the geometric limits

$$0.3 \le a/R \le 0.8\ , \quad 0.55 \le a/c \le 0.75$$

we restricted the computations on this area. For the computations we used ABAQUS Version 6.9 on a mesh of 3100 elements and 14800 nodes. The cylinder length was chosen $2H$=20 R and 1/4th of the whole specimen was modelled.

FE-results are shown in Fig. 4a for a few geometries and ν=0.3. They are in suitable agreement with the fitting equation provided in [3]. In this context, it should be mentioned that the Body Force Method shows a higher accuracy than FE-computations. The variation of stress intensity factor along the coordinate x (Fig. 2a) is shown in Fig. 4b for a/c=0.3 via the geometric function F. Only negligible variation is visible. In contrast to this finding, the deep crack shows increasing stress intensity to the surface. Figure 4c shows a comparison of geometric functions normalized on their value at point (A). Note that in this case the abscissa is changed.

Figure 5 shows the effect of the Poisson's ratio on the stress intensity factor for two crack geometries by plotting the geometric functions for several values of ν, normalized on the geometric function at ν=0.3. At point (A) the stress intensity factor for ν=0.17 is 3% smaller than for ν=0.3. In contrast a variation on ν is negligible at point (C).

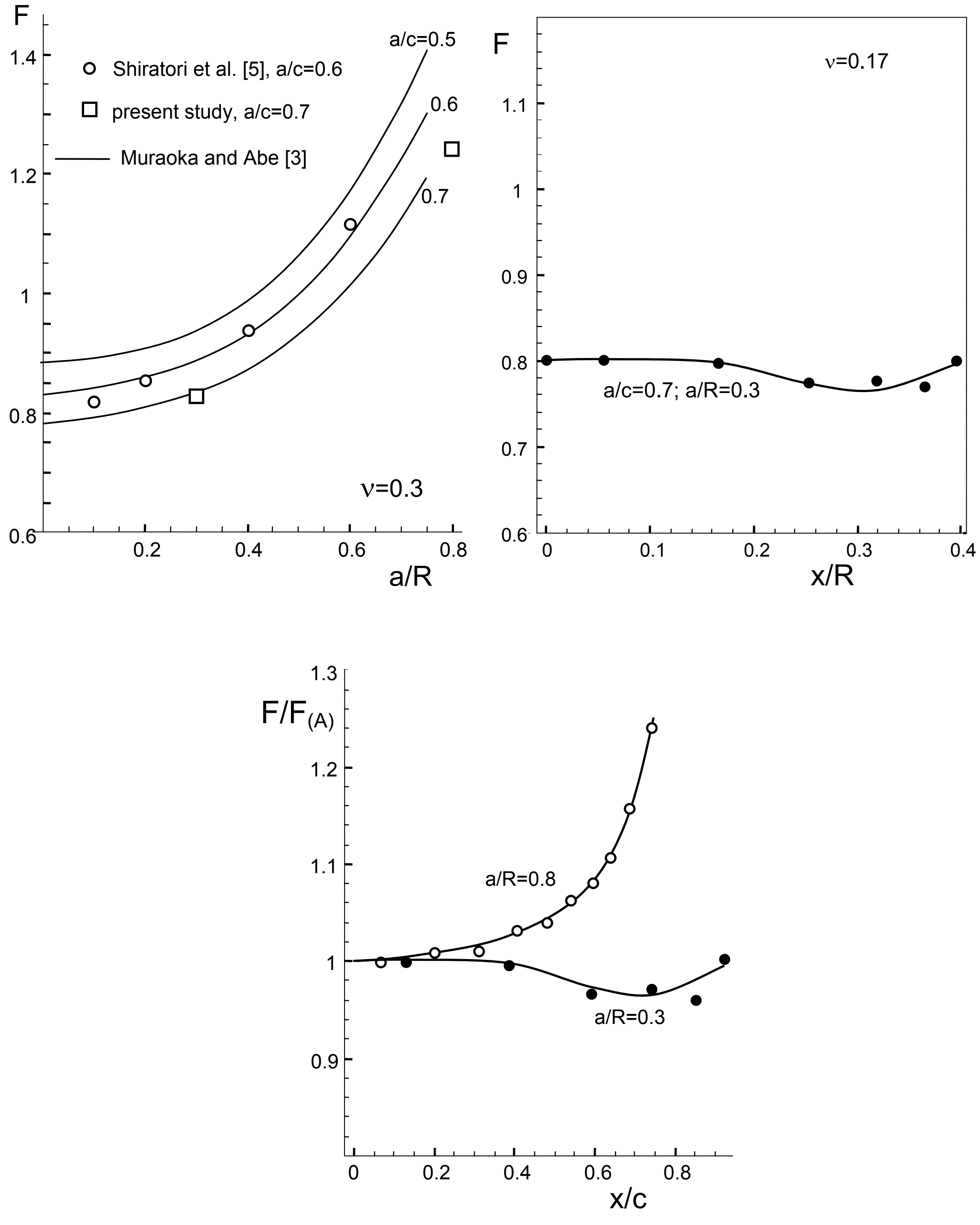

Fig. 4 a) FE-results compared with the equation in [3] for ν=0.3, b) variation of *F* along the crack front for ν=0.17, c) geometric functions normalized on the value at point (A).

The relation between energy release rate, *G*, and stress intensity factor, *K*, yields for plane strain conditions

$$K^2 = G\frac{E}{1-\nu^2} \Rightarrow K \propto \frac{1}{\sqrt{1-\nu^2}} \tag{2}$$

This dependency is represented in Fig. 5 by the dashed curve. It should be noted that the case ν=0 reflects plane stress conditions. The variation of stress intensity factor with ν indicates that plane strain conditions are predominantly fulfilled at point (A). At the surface point (C) we nearly have plane stress conditions already due to the geometry.

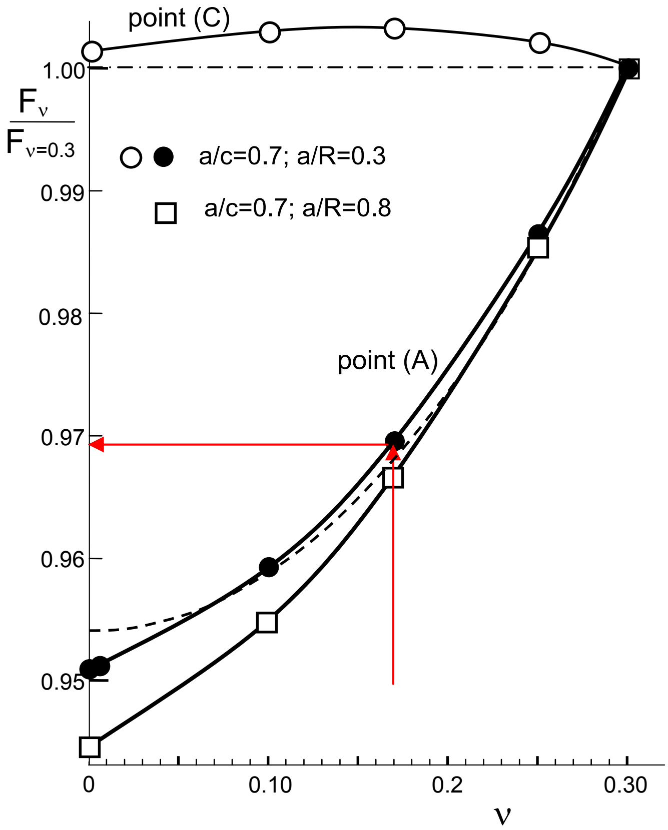

Fig. 5 Effect of Poisson's ratio on stress intensity factors, dashed line: trend by eq.(2).

Due to eq.(2) the stress intensity factor for 0.15≤ν≤0.3 can be approximated by

$$K(\nu) \cong K(0.3)\frac{0.954}{\sqrt{1-\nu^2}} \tag{3}$$

showing deviations less than 0.2%.

4. T-stress

The first higher-order stress term of the crack-tip stress field is the so-called T-stress. It is defined as the only existing component of the stress tensor

$$\sigma_{ij,0} = \begin{pmatrix} \sigma_{xx,0} & 0 \\ 0 & 0 \end{pmatrix} \underset{def}{\equiv} \begin{pmatrix} T & 0 \\ 0 & 0 \end{pmatrix} \tag{4}$$

According to the suggestion by Leevers and Radon [7] we use the dimensionless representation of T by the stress biaxiality ratio β, defined as

$$\beta = \frac{T\sqrt{\pi a}}{K_I} \tag{5}$$

The variation of β along the crack front is shown in Fig. 6 for differently deep cracks. Figure 7 shows the effect of ν on T-stress and biaxiality ratio β.

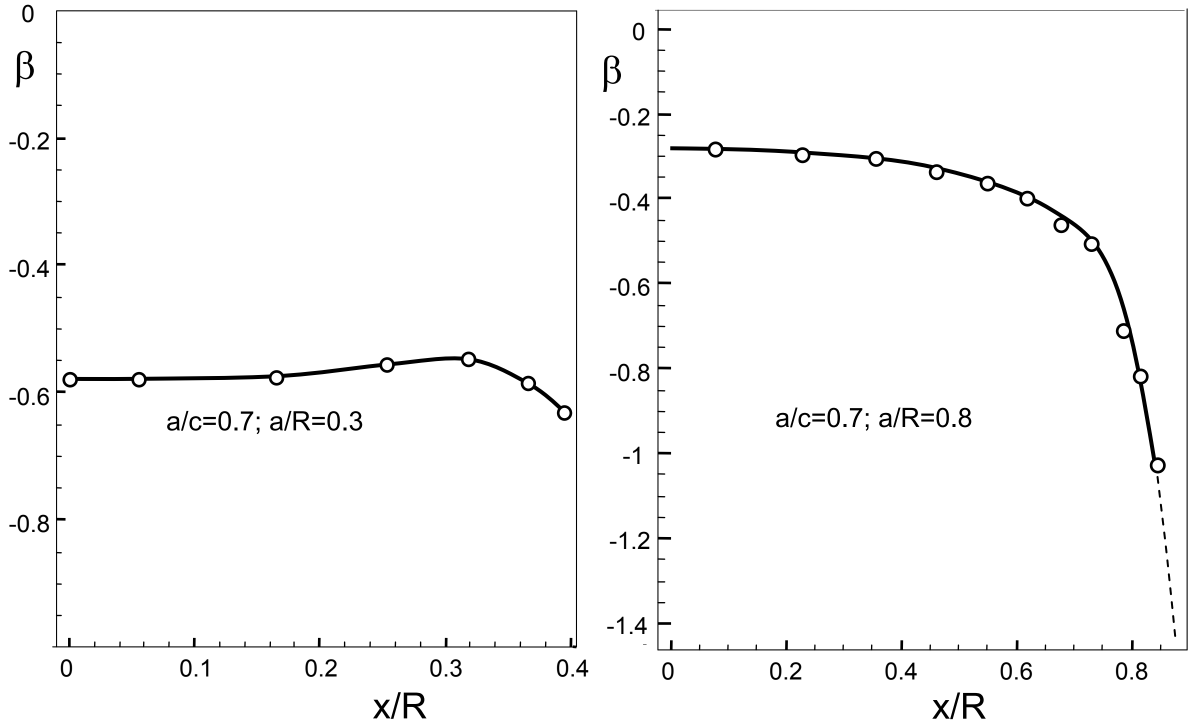

Fig. 6 Variation of β along the crack front.

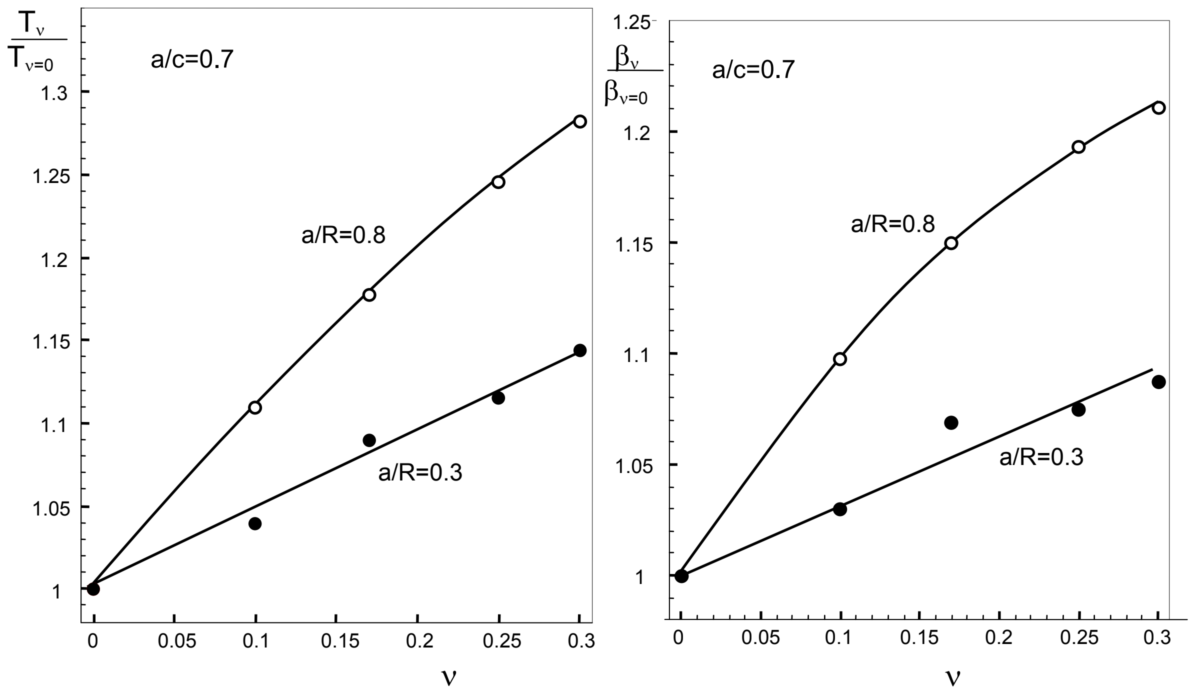

Fig. 7 Effect of Poisson's ratio on a) T-stress and b) biaxiality ratio.

5. Correction of subcritical crack growth data

Finally, the subcritical crack growth curve from Muraoka and Abe [3] is re-plotted by using the stress intensity factors for ν=0.17. Figure 8 shows the result. In the region 10^{-9}m/s≤v≤10^{-6} m/s, the re-evaluated data from Muraoka and Abe [3] are in best agreement with the data by Wiederhorn and Bolz [1].

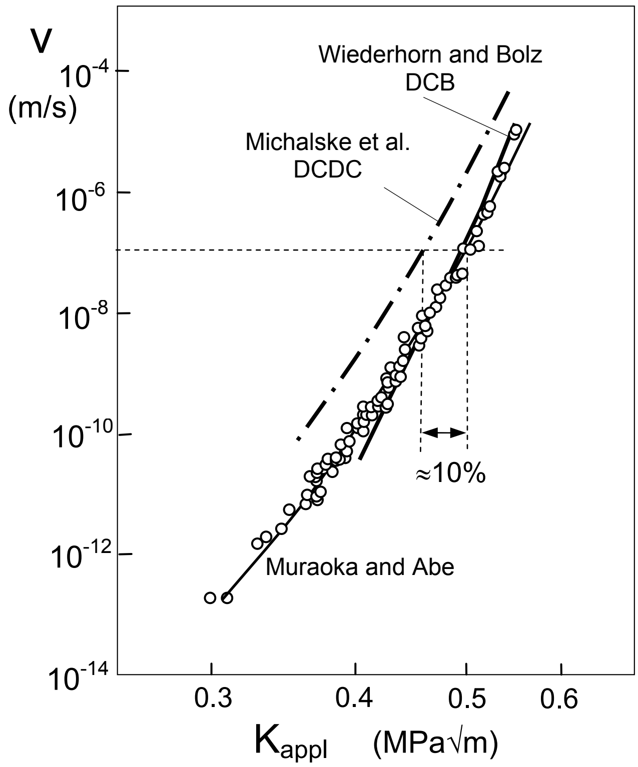

Fig. 8 Re-evaluated data by Muraoka and Abe [3] compared with data from straight cracks.

References

1 S.M. Wiederhorn and L.H. Bolz, Stress Corrosion and Static Fatigue of Glass, J. Am. Ceram. Soc. **53**(1970) 543-548.

2 Michalske, T.A., Smith, W.L., Bunker, B.C., Fatigue mechanisms in high-strength silica-glass fibers, J. Am. Ceram. Soc., **74**(1991), 1993-96.

3 M. Muraoka and H. Abé, “Subcritical Crack Growth in silica Optical Fibers in a Wide Range of Crack Velocities,” J. Am. Ceram. Soc. **79**(1996), 51-57.

4 H. Nisitani, D.H. Chen, Stress intensity factor for a semi-elliptic surface crack in a shaft under tension, Trans. Japan Soc. Mech. Engrs., Vol 50, No. 453(1984), 1077-1082.

5 M. Shiratori, T. Miyoshi, Y. Sakai, G.R. Zhang, Analysis of stress intensity factors subjected to arbitrarily distributed surface stresses, Trans. Japan Soc. Mech. Engnrs (1986).

6 M. Muraoka, personal communication 2015.

7 Leevers, P.S., Radon, J.C., Inherent stress biaxiality in various fracture specimen geometries, Int. J. Fract. **19**(1982), 311-325.

KIT Scientific Working Papers
ISSN 2194-1629